20 Water tube system

20.1 General information

This IVP is an index 2 system of 49 non-linear Differential-Algebraic Equations and describes the water flow through a tube system, taking into account turbulence and the roughness of the tube walls. The parallel-IVP-algorithm group of CWI contributed this problem to the test set in cooperation with B. Koren (CWI) and Paragon Decision Technology B.V.

The software part of the problem is in the file water.f available at [MM08].

20.2 Mathematical description of the problem

The problem is of the form

$$M\frac{\mathrm{d}y}{\mathrm{d}t} = f(t,y), \qquad y(0)=y_0, \quad y'(0)=y'_0, \tag{II.20.1}$$

where $0 \le t \le 17\cdot 3600$ and $y \in \mathbb{R}^{49}$. Furthermore,

$$M = \begin{bmatrix} M^\phi & O & O \\ O & O & O \\ O & O & M^p \end{bmatrix}, \tag{II.20.2}$$

where $M^\phi \in \mathbb{R}^{18\times 18}$ and $M^p \in \mathbb{R}^{13\times 13}$ are given by

$$M^\phi_{i,j} = \begin{cases} v_i & \text{for } i=j, \\ 0 & \text{otherwise.} \end{cases} \qquad M^p_{i,j} = \begin{cases} C_5 & \text{for } i=j=1, \\ C_8 & \text{for } i=j=2, \\ 0 & \text{otherwise,} \end{cases}$$

The first 38 components of y are of index 1, the last 11 are of index 2. For the definition of f and the values of C_5, C_8 and v we refer to §20.3.

The initial vectors y_0 and y'_0 are given by

$$y_0 = \begin{cases} 0 & \text{for} \quad i=1,2,\ldots,18 \\ 0.047519404529185289807 & \text{for} \quad i=19,20,\ldots,36 \\ 109800 & \text{for} \quad i=37,38,\ldots,49 \end{cases} \quad \text{and} \quad y'_0 = (0,\ldots,0)^{\mathrm{T}}. \tag{II.20.3}$$

The function f contains several square roots. It is clear that the function can not be evaluated if one of the arguments of one of these square roots becomes negative. To prevent this situation, we set `IERR=-1` in the Fortran subroutine that defines f if this happens. See page *IV-ix* of the the description of the software part of the test set for more details on `IERR`.

20.3 Origin of the problem

This test example describes how water flows through a water tube system. The system is represented by a set of nodes, which are connected by tubes. The structure of the water tube system is depicted in Figure II.20.1. There are two types of nodes: normal nodes and buffer nodes, to which a buffer is attached. We denote the set of all nodes by $\mathcal{N}$, and the set of buffer nodes by $\mathcal{B}$. For the system under consideration, $\mathcal{B} = \{5, 8\}$. The rectangles in Figure II.20.1 represent the buffers. The pipes are in the horizontal plane; the buffers are connected to the nodes perpendicular to this plane. The pipes from the buffer nodes to the rectangles are virtual; in reality the buffers are directly attached to the buffer nodes. In the model every node can have inflow and outflow, which are denoted by $e_i^{\mathrm{in}}(t)$ and $e_i^{\mathrm{out}}(t)$. In our example, inflow occurs only at node 1 and node 13, whereas only node 10 has outflow.

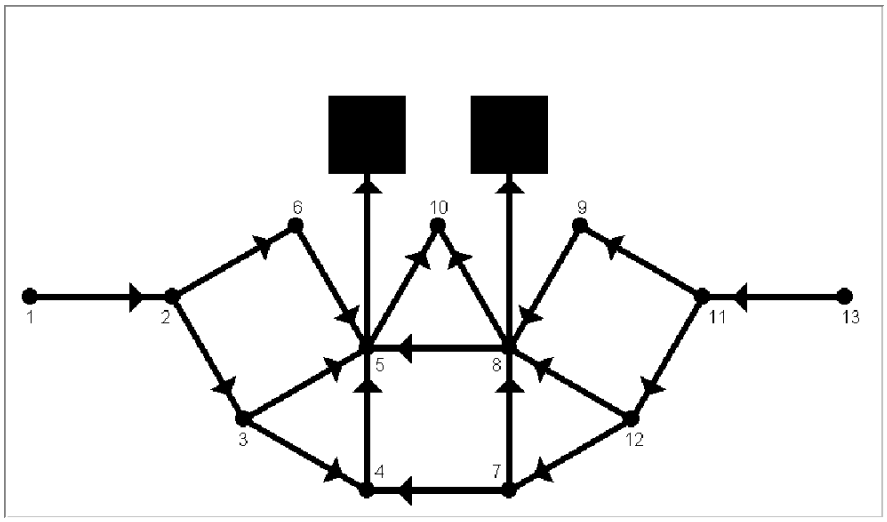

FIGURE II.20.1: *Structure of water tube system.*

The unit of time in the model is second. Defining the time in hours by $\hat{t} = t/3600$, these flows are defined by

$$\begin{aligned} e_1^{\text{in}}(t) &= (1 - \cos(\mathrm{e}^{-\hat{t}} - 1))/200, \\ e_{13}^{\text{in}}(t) &= (1 - \cos(\mathrm{e}^{-\hat{t}} - 1))/80, \\ e_{10}^{\text{out}}(t) &= \hat{t}^2(3\hat{t}^2 - 92\hat{t} + 720)/10^6. \end{aligned}$$

Figure II.20.2 shows plots of these flows as function of $\hat{t}$. Note that the outflow has a peak at 8 AM and is increasing again after 3 PM.

Although it seems that node 6 and node 9 could be omitted, we include them in the model, to leave open the possibility that these nodes have inflow or outflow. The arrows in Figure II.20.1 denote the direction in which we compute the flows. For example, if there is a flow from node 4 to node 3, then this flow will be negative.

To model the flow of the water, we introduce some symbols, which are listed in Table II.20.1. The roughness $k_{i,j} = 2 \cdot 10^{-4}$ is measured as the average height of the obstacles on the tube wall. The structure $S_{i,j}$ is defined as

$$S_{i,j} = \begin{cases} 1 & \text{if there is a tube from } i \text{ to } j, \\ 0 & \text{otherwise.} \end{cases}$$

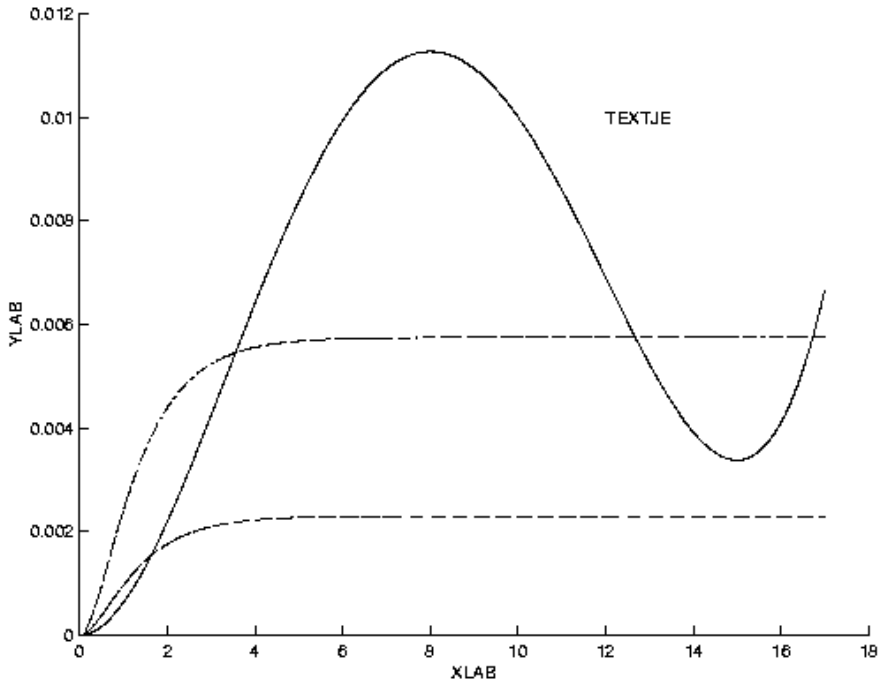

FIGURE II.20.2: *Inflows and outflow in m^3/s as function of time in hours.*

From Figure II.20.1 we see that

$$S = \begin{bmatrix} 0 & 1 & 0 & 0 & 0 & 0 & 0 & 0 & 0 & 0 & 0 & 0 & 0 \\ 0 & 0 & 1 & 0 & 0 & 1 & 0 & 0 & 0 & 0 & 0 & 0 & 0 \\ 0 & 0 & 0 & 1 & 1 & 0 & 0 & 0 & 0 & 0 & 0 & 0 & 0 \\ 0 & 0 & 0 & 0 & 1 & 0 & 0 & 0 & 0 & 0 & 0 & 0 & 0 \\ 0 & 0 & 0 & 0 & 0 & 0 & 0 & 0 & 0 & 1 & 0 & 0 & 0 \\ 0 & 0 & 0 & 0 & 1 & 0 & 0 & 0 & 0 & 0 & 0 & 0 & 0 \\ 0 & 0 & 0 & 1 & 0 & 0 & 0 & 1 & 0 & 0 & 0 & 0 & 0 \\ 0 & 0 & 0 & 0 & 1 & 0 & 0 & 0 & 0 & 1 & 0 & 0 & 0 \\ 0 & 0 & 0 & 0 & 0 & 0 & 0 & 1 & 0 & 0 & 0 & 0 & 0 \\ 0 & 0 & 0 & 0 & 0 & 0 & 0 & 0 & 0 & 0 & 0 & 0 & 0 \\ 0 & 0 & 0 & 0 & 0 & 0 & 0 & 0 & 1 & 0 & 0 & 1 & 0 \\ 0 & 0 & 0 & 0 & 0 & 0 & 1 & 1 & 0 & 0 & 1 & 0 & 0 \\ 0 & 0 & 0 & 0 & 0 & 0 & 0 & 0 & 0 & 0 & 1 & 0 & 0 \end{bmatrix}.$$

Some of the quantities in Table II.20.1 can be computed directly from others:

$$\begin{aligned} \mu &= \nu \cdot \rho, \\ \phi_{i,j}(t) &= u_{i,j}(t) \cdot A_{i,j}, \\ A_{i,j} &= \pi \cdot d_{i,j}^2/4, \\ m_{i,j} &= A_{i,j} \cdot l_{i,j} \cdot \rho, \\ R_{i,j}(t) &= u_{i,j}(t) \cdot d_{i,j}/\nu. \end{aligned}$$

The definition of $R_{i,j}(t)$ was taken from [Sch78, p. 816].

TABLE II.20.1: *List of symbols for modeling flow in tubes.*

Symbol	Unit	Meaning
$\phi_{i,j}(t)$	m^3/s	flow through tube from i to j at time t
$u_{i,j}(t)$	m/s	mean velocity of flow through tube from i to j at time t
$F_{i,j}(t)$	N	total force on water in tube from i to j at time t
$F^{\mathrm{a}}_{i,j}(t)$	N	adhesion force on water in tube from i to j at time t
$\lambda_{i,j}(t)$	-	coefficient of resistance of tube from i to j at time t
$R_{i,j}(t)$	-	Reynolds number of flow through tube from i to j at time t
$p_i(t)$	N/m^2	pressure in i at time t
$S_{i,j}$	-	incidence matrix for structure of the tube system
$m_{i,j}$	kg	mass of water in tube from i to j
$d_{i,j}$	m	diameter of tube from i to j
$l_{i,j}$	m	length of tube from i to j
$A_{i,j}$	m^2	area of tube from i to j
$k_{i,j}$	m	roughness of wall of tube from i to j
$e^{\mathrm{in}}_i(t)$	m^3/s	inflow at i at time t
$e^{\mathrm{out}}_i(t)$	m^3/s	outflow at i at time t
B_i $(i \in \mathcal{B})$	m^2	area of buffer i
R^{crit}	-	critical Reynolds number
g	m/s^2	gravity constant
ρ	kg/m^3	density of water
μ	$kg/(m \cdot s)$	viscosity of water
ν	m^2/s	kinematic viscosity of water
v	kg/m^4	auxiliary vector, see (II.20.15)

We now explain how to model the flow through a tube, using Newton's second Law, which states that

$$m_{i,j}\frac{\mathrm{d}u_{i,j}(t)}{\mathrm{d}t} = F_{i,j}(t). \tag{II.20.4}$$

Assuming that gravity has no influence on the water flow in all tubes (remember that the pipes are in the horizontal plane), we see from Figure II.20.3 that the total force on the water in a tube equals

$$F_{i,j}(t) = A_{i,j}(p_i(t) - p_j(t)) - F^{\mathrm{a}}_{i,j}(t). \tag{II.20.5}$$

The magnitude of the adhesion force depends on the type of flow. For laminar flows ($|R_{i,j}(t)| \leq R^{\mathrm{crit}}$), we use the formula [Sch78, p. 12]

$$F^{\mathrm{a}}_{i,j}(t)/A_{i,j} = 32\mu \cdot l_{i,j} \cdot u_{i,j}(t)/d^2_{i,j}. \tag{II.20.6}$$

For turbulent flows ($|R_{i,j}(t)| > R^{\mathrm{crit}}$), we have [Sch78, p. 597]

$$F^{\mathrm{a}}_{i,j}(t)/A_{i,j} = \lambda_{i,j}(t) \cdot \rho \cdot l_{i,j} \cdot u_{i,j}(t)^2/d_{i,j}, \tag{II.20.7}$$

where the resistance $\lambda_{i,j}(t)$ is computed from Colebrook and White's formula [Sch78, p. 621]:

$$0 = \frac{1}{\sqrt{\lambda_{i,j}(t)}} - 1.74 + 2\log\left(\frac{2k_{i,j}}{d_{i,j}} + \frac{18.7}{|R_{i,j}(t)|\sqrt{\lambda_{i,j}(t)}}\right). \tag{II.20.8}$$

Although for laminar flows the adhesion force does not depend on the resistance coefficient (cf. (II.20.6)), we have to choose a value for $\lambda_{i,j}$ in case of laminar flows. We compute this value by

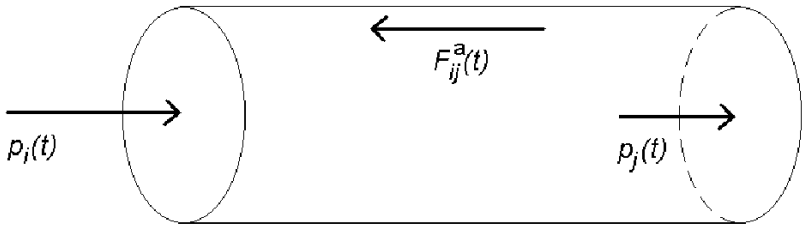

FIGURE II.20.3: *Forces on water in tube.*

replacing $R_{i,j}$ in (II.20.8) by R^{crit}, i.e., we choose the value such that if a flow changes from laminar into turbulent, the resistance coefficient changes gradually.

For the normal nodes, Kirchoff's law holds, which states that

$$\forall\, n \in \mathcal{N} - \mathcal{B}: \qquad 0 = \sum_{i|S_{i,n}=1} \phi_{i,n}(t) + e_n^{\text{in}}(t) - \sum_{j|S_{n,j}=1} \phi_{n,j}(t) - e_n^{\text{out}}(t) \tag{II.20.9}$$

For the buffer nodes, we add a term $\psi_n(t)$ that represents the flow to the buffer:

$$\forall\, n \in \mathcal{B}: \qquad \psi_n(t) = \sum_{i|S_{i,n}=1} \phi_{i,n}(t) + e_n^{\text{in}}(t) - \sum_{j|S_{n,j}=1} \phi_{n,j}(t) - e_n^{\text{out}}(t) \tag{II.20.10}$$

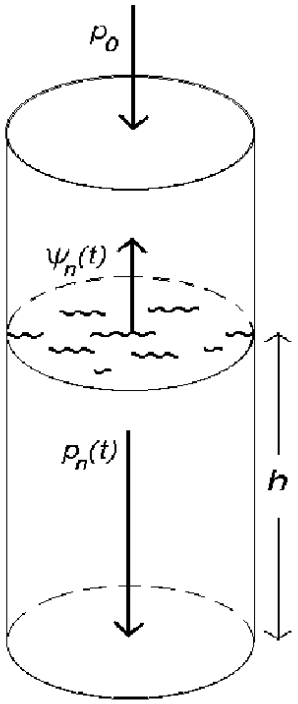

FIGURE II.20.4: *Representation of water buffer.*

We now explain how to compute $\psi_n(t)$. A buffer can be interpreted as the water column in Figure II.20.4, with ground area B_n and height h. Due to the flow $\psi_n(t)$ the height of the buffer changes at a rate $\psi_n(t)/B_n$. The difference between the pressure at the top and bottom of the column satisfies

$$p_n - p_0 = g \cdot \rho \cdot h.$$

Consequently, the pressure difference changes at a rate given by

$$\frac{\mathrm{d}(p_n - p_0)}{\mathrm{d}t} = g \cdot \rho \cdot \frac{\mathrm{d}h}{\mathrm{d}t} = g \cdot \rho \cdot \frac{\psi_n(t)}{B_n}. \tag{II.20.11}$$

Notice that the pressure p_0 is constant and therefore drops out in this formula. Substituting (II.20.11) in (II.20.10) gives

$$\forall\, n \in \mathcal{B}: \qquad C_n \frac{\mathrm{d}p_n(t)}{\mathrm{d}t} = \sum_{i|S_{i,n}=1} \phi_{i,n}(t) + e_n^{\mathrm{in}}(t) - \sum_{j|S_{n,j}=1} \phi_{n,j}(t) - e_n^{\mathrm{out}}(t), \tag{II.20.12}$$

where the quantity $C_n := B_n/(\rho \cdot g)$ can be interpreted as the capacity of the buffer at node n.

We arrive at the formulation in §20.2 by setting

$$\begin{aligned} y = (\quad & \phi_{1,2}(t), \phi_{2,3}(t), \phi_{2,6}(t), \phi_{3,4}(t), \phi_{3,5}(t), \phi_{4,5}(t), \phi_{5,10}(t), \phi_{6,5}(t), \phi_{7,4}(t), \\ & \phi_{7,8}(t), \phi_{8,5}(t), \phi_{8,10}(t), \phi_{9,8}(t), \phi_{11,9}(t), \phi_{11,12}(t), \phi_{12,7}(t), \phi_{12,8}(t), \phi_{13,11}(t), \\ & \lambda_{1,2}(t), \lambda_{2,3}(t), \lambda_{2,6}(t), \lambda_{3,4}(t), \lambda_{3,5}(t), \lambda_{4,5}(t), \lambda_{5,10}(t), \lambda_{6,5}(t), \lambda_{7,4}(t), \\ & \lambda_{7,8}(t), \lambda_{8,5}(t), \lambda_{8,10}(t), \lambda_{9,8}(t), \lambda_{11,9}(t), \lambda_{11,12}(t), \lambda_{12,7}(t), \lambda_{12,8}(t), \lambda_{13,11}(t), \\ & p_5(t), p_8(t), p_1(t), p_2(t), \ldots, p_4(t), p_6(t), p_7(t), p_9(t), p_{10}(t), \ldots, p_{13}(t) \qquad)^{\mathrm{T}}. \end{aligned} \tag{II.20.13}$$

All pressures are of index 2, except for those at the buffer nodes. The reordering of the pressures in (II.20.13) is such that the elements in y appear in order of increasing index, as required by RADAU, RADAU5 and MEBDFDAE.

The first 18 equations in (II.20.1) are obtained by first substituting (II.20.5) in (II.20.4). Next, we divide both sides by $A_{i,j}$, thus yielding

$$\frac{\rho \cdot l_{i,j}}{A_{i,j}} \frac{\mathrm{d}\phi_{i,j}(t)}{\mathrm{d}t} = p_i(t) - p_j(t) - F_{i,j}^{\mathrm{a}}(t)/A_{i,j}. \tag{II.20.14}$$

Finally, (II.20.6) and (II.20.7) are substituted in (II.20.14). Consequently, if we define $V_{i,j} = \rho \cdot l_{i,j}/A_{i,j}$, then the vector v in (II.20.2) is given by

$$\begin{aligned} v = (\quad & V_{1,2}, V_{2,3}, V_{2,6}, V_{3,4}, V_{3,5}, V_{4,5}, V_{5,10}, V_{6,5}, V_{7,4}, \\ & V_{7,8}, V_{8,5}, V_{8,10}, V_{9,8}, V_{11,9}, V_{11,12}, V_{12,7}, V_{12,8}, V_{13,11} \quad)^{\mathrm{T}}. \end{aligned} \tag{II.20.15}$$

The next 18 equations in (II.20.1) equal (II.20.8), whereas the last 13 equations are given by (II.20.9) and (II.20.12).

In this model, all tubes and buffers are equal with characteristics as specified in Table II.20.2. Moreover, we assume that the temperature is constant. The values for the physical constants are listed in Table II.20.3. The values for ρ and ν correspond to a temperature of 10°C. The value for R^{crit} was taken from [Sch78, p. 39].

We now discuss how we derived the initial conditions in (II.20.3). First we note that (II.20.9) is an index 2 constraint. Therefore, the initial values also have to satisfy the once differentiated constraint (the so-called *hidden* constraint)

$$\forall\, n \in \mathcal{N} - \mathcal{B}: \qquad 0 = \sum_{i|S_{i,n}=1} \phi'_{i,n}(t) + e_n^{\mathrm{in}\prime}(t) - \sum_{j|S_{n,j}=1} \phi'_{n,j}(t) - e_n^{\mathrm{out}\prime}(t). \tag{II.20.16}$$

TABLE II.20.2: *Characteristics of tubes.*

Quantity	Value
$l_{i,j}$	1000
$k_{i,j}$	0.0002
$d_{i,j}$	1
B_i	200

TABLE II.20.3: *Values of physical constants.*

Constant	Value
ν	$1.31 \cdot 10^{-6}$
g	9.8
ρ	$1.0 \cdot 10^{3}$
R^{crit}	$2.3 \cdot 10^{3}$

We are free to choose initial flows $\phi_{i,j}(0)$ as long as they satisfy (II.20.9); we chose these all equal to zero. This means that the resistance coefficients equal the value for the case of laminar flows, i.e., 0.047519... The pressures at the buffer nodes, which can be selected freely, are chosen to be $10^5 + g \cdot \rho$, which corresponds to initial heights of one meter in the water columns, assuming that p_0 in Figure II.20.4 equals one bar. From (II.20.12) it follows that $p'_n(0) = 0$, $n \in \mathcal{B}$ (note that the in- and outflows are initially zero). The initial pressures $p_n(0)$, $n \in \mathcal{N} - \mathcal{B}$, and the initial derivative flows $\phi'_{i,j}(0)$ follow from (II.20.14) and (II.20.16). Since the derivatives of the in- and outflows are initially zero, the initial values in (II.20.3) satisfy these equations. The other initial values, $\lambda'_{i,j}(0)$ and $p'_n(0)$, $n \in \mathcal{N} - \mathcal{B}$, appear neither in the system, nor in the hidden constraints, and can be chosen freely. We set these equal to 0.

Several observations can be made from the behavior of the flows, resistance coefficients and pressures, which are plotted in Figure II.20.6–II.20.8:

- The rise and fall of the outflow in node 10 cause the flows to node 10 to change from laminar to turbulent and back, as can be seen from the resistance coefficients $\lambda_{5,10}$ and $\lambda_{8,10}$, which correspond to y_{25} and y_{30}.
- At 8 AM, the pressures in the buffer nodes drop below their original level, which means that some of the water that was present in the buffers initially, is used to meet the peak demand.
- The time period in which the flows to node 10 have become laminar again (this period is indicated by the vertical dashed lines in the plots of y_{25} and y_{30}, causes an irregular behavior (indicated again by dashed lines) of the solution components y_3, y_6, y_9, y_{10} and y_{11} which correspond to the flow from node 3 to node 4 and the flows in the cycle 4–7–8–5, respectively.
- Some of the flows contain high-frequent oscillations of small amplitude. To see this more clearly, we plotted $\phi_{3,4}$ for $6878 < t \leq 17 \cdot 3600$ in Figure II.20.5.

20.4 Numerical solution of the problem

Tables II.20.4–II.20.5 and Figures II.20.6–II.20.8 present the reference solution at the end of the integration interval, the run characteristics, the behavior of the solution over the integration interval and the work-precision diagrams, respectively.

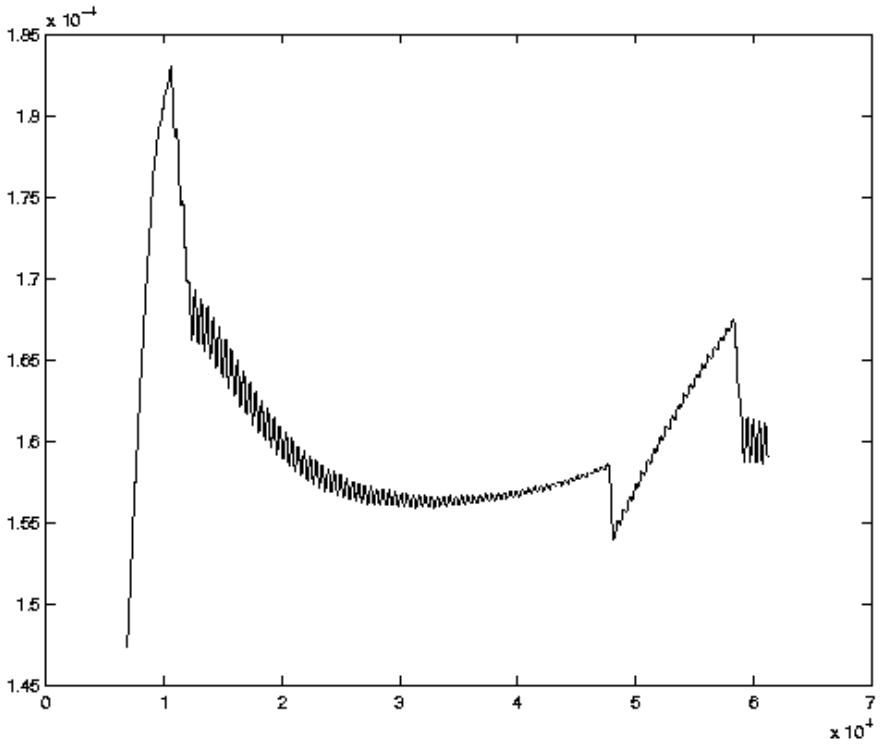

FIGURE II.20.5: *Behavior of* $\phi_{3,4}$ *for* $6878 < t \leq 17 \cdot 3600$.

Since the 13 last solution components (the pressures) are so much larger in magnitude than the other components, we used the following vector-valued input tolerances:

$$\begin{array}{ll} \text{atol}(i) = \text{atol} & \text{for } i = 1, \ldots, 36, \\ \text{atol}(i) = 10^6 \cdot \text{atol} & \text{for } i = 37, \ldots, 49, \\ \text{rtol}(i) = \text{rtol} & \text{for } i = 1, \ldots, 49. \end{array}$$

The reference solution was computed by PSIDE with `rtol = atol` $= 10^{-14}$. For the work-precision diagrams, we used: rtol $= 10^{-(4+m/4)}$, $m = 0, 1, \ldots, 24$; atol = rtol; h0 = rtol for BIMD, GAMD, MEBDFDAE, MEBDFI, RADAU and RADAU5.

The failed runs are in Table II.20.6; listed are the name of the solver that failed, for which values of m this happened, and the reason for failing.

.

References

[MM08] F. Mazzia and C. Magherini. *Test Set for Initial Value Problem Solvers, release 2.4.* Department of Mathematics, University of Bari and INdAM, Research Unit of Bari, February 2008. Available at http://www.dm.uniba.it/~testset.

[Sch78] H. Schlichting. *Boundary-Layer Theory.* Series in mechanical engineering. Mc Graw-Hill, seventh edition, 1978.

TABLE II.20.4: *Reference solution at the end of the integration interval.*

y_1	$0.2298488296477430 \cdot 10^{-002}$	y_{26}	$0.4751940452918529 \cdot 10^{-001}$
y_2	$0.1188984650746585 \cdot 10^{-002}$	y_{27}	$0.4751940452918529 \cdot 10^{-001}$
y_3	$0.1109503645730845 \cdot 10^{-002}$	y_{28}	$0.4751940452918529 \cdot 10^{-001}$
y_4	$0.1589620100314825 \cdot 10^{-003}$	y_{29}	$0.4751940452918529 \cdot 10^{-001}$
y_5	$0.1030022640715102 \cdot 10^{-002}$	y_{30}	$0.4249217433601160 \cdot 10^{-001}$
y_6	$0.8710606306836165 \cdot 10^{-003}$	y_{31}	$0.4732336439609648 \cdot 10^{-001}$
y_7	$0.3243571480903489 \cdot 10^{-002}$	y_{32}	$0.4732336439609648 \cdot 10^{-001}$
y_8	$0.1109503645730845 \cdot 10^{-002}$	y_{33}	$0.4270002118868241 \cdot 10^{-001}$
y_9	$0.7120986206521341 \cdot 10^{-003}$	y_{34}	$0.4751940452918529 \cdot 10^{-001}$
y_{10}	$0.6414613963833099 \cdot 10^{-003}$	y_{35}	$0.4751940452918529 \cdot 10^{-001}$
y_{11}	$0.9416978549524347 \cdot 10^{-003}$	y_{36}	$0.3651427026675656 \cdot 10^{-001}$
y_{12}	$0.3403428519096511 \cdot 10^{-002}$	y_{37}	$0.1111268591478108 \cdot 10^{+006}$
y_{13}	$0.2397639310739395 \cdot 10^{-002}$	y_{38}	$0.1111270045592387 \cdot 10^{+006}$
y_{14}	$0.2397639310739395 \cdot 10^{-002}$	y_{39}	$0.1111271078730254 \cdot 10^{+006}$
y_{15}	$0.3348581430454180 \cdot 10^{-002}$	y_{40}	$0.1111269851929858 \cdot 10^{+006}$
y_{16}	$0.1353560017035444 \cdot 10^{-002}$	y_{41}	$0.1111269255355337 \cdot 10^{+006}$
y_{17}	$0.1995021413418736 \cdot 10^{-002}$	y_{42}	$0.1111269322658045 \cdot 10^{+006}$
y_{18}	$0.5746220741193575 \cdot 10^{-002}$	y_{43}	$0.1111269221703983 \cdot 10^{+006}$
y_{19}	$0.4751940452918529 \cdot 10^{-001}$	y_{44}	$0.1111270121140691 \cdot 10^{+006}$
y_{20}	$0.4751940452918529 \cdot 10^{-001}$	y_{45}	$0.1111274419515807 \cdot 10^{+006}$
y_{21}	$0.4751940452918529 \cdot 10^{-001}$	y_{46}	$0.1111255158881087 \cdot 10^{+006}$
y_{22}	$0.4751940452918529 \cdot 10^{-001}$	y_{47}	$0.1111278793439227 \cdot 10^{+006}$
y_{23}	$0.4751940452918529 \cdot 10^{-001}$	y_{48}	$0.1111270995171642 \cdot 10^{+006}$
y_{24}	$0.4751940452918529 \cdot 10^{-001}$	y_{49}	$0.1111298338971779 \cdot 10^{+006}$
y_{25}	$0.4311196778792902 \cdot 10^{-001}$		

TABLE II.20.5: *Run characteristics.*

solver	rtol	atol	h0	mescd	scd	steps	accept	#f	#Jac	#LU	CPU
BIMD	10^{-4}	10^{-4}	10^{-4}	3.55	1.23	17	16	250	16	17	0.0420
	10^{-7}	10^{-7}	10^{-7}	6.05	3.45	333	314	5830	314	333	0.8989
	10^{-10}	10^{-10}	10^{-10}	9.22	7.32	673	586	17454	586	673	2.1101
GAMD	10^{-4}	10^{-4}	10^{-4}	3.51	1.18	18	16	340	16	18	0.0439
	10^{-7}	10^{-7}	10^{-7}	5.94	3.40	233	202	8038	204	233	0.7642
	10^{-10}	10^{-10}	10^{-10}	9.32	7.18	554	458	22918	448	536	1.9744
MEBDFI	10^{-4}	10^{-4}	10^{-4}	3.85	1.83	81	77	1197	18	18	0.0488
	10^{-7}	10^{-7}	10^{-7}	6.32	3.30	1267	1171	13926	192	192	0.5846
	10^{-10}	10^{-10}	10^{-10}	9.09	7.18	3189	3037	28403	351	351	1.2561
PSIDE-1	10^{-4}	10^{-4}		4.37	2.45	64	50	799	16	244	0.1015
	10^{-7}	10^{-7}		5.80	3.09	134	104	2320	40	468	0.2723
	10^{-10}	10^{-10}		7.86	5.45	827	719	14105	39	1292	1.2102

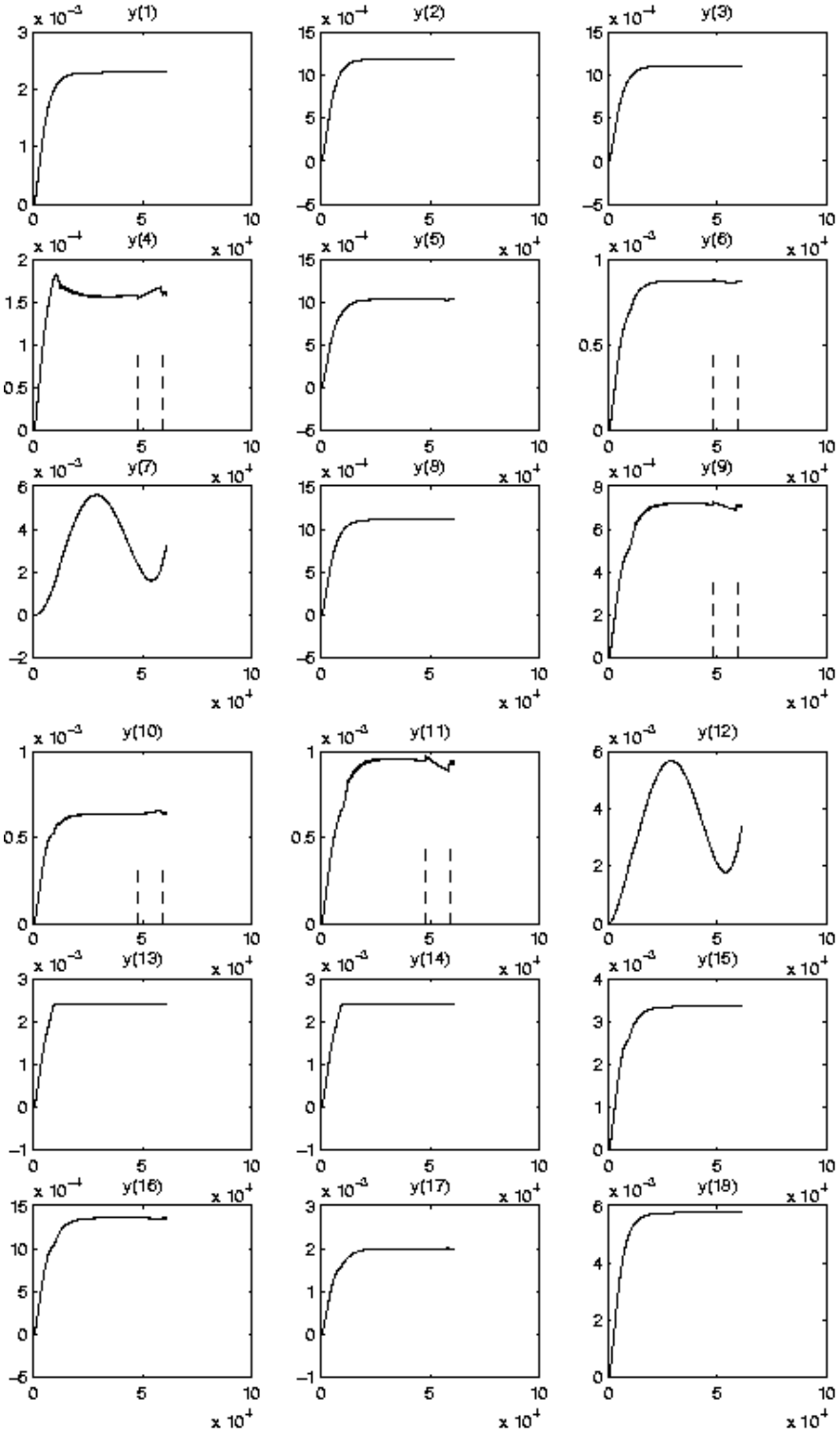

FIGURE II.20.6: *Behavior of flows over the integration interval.*

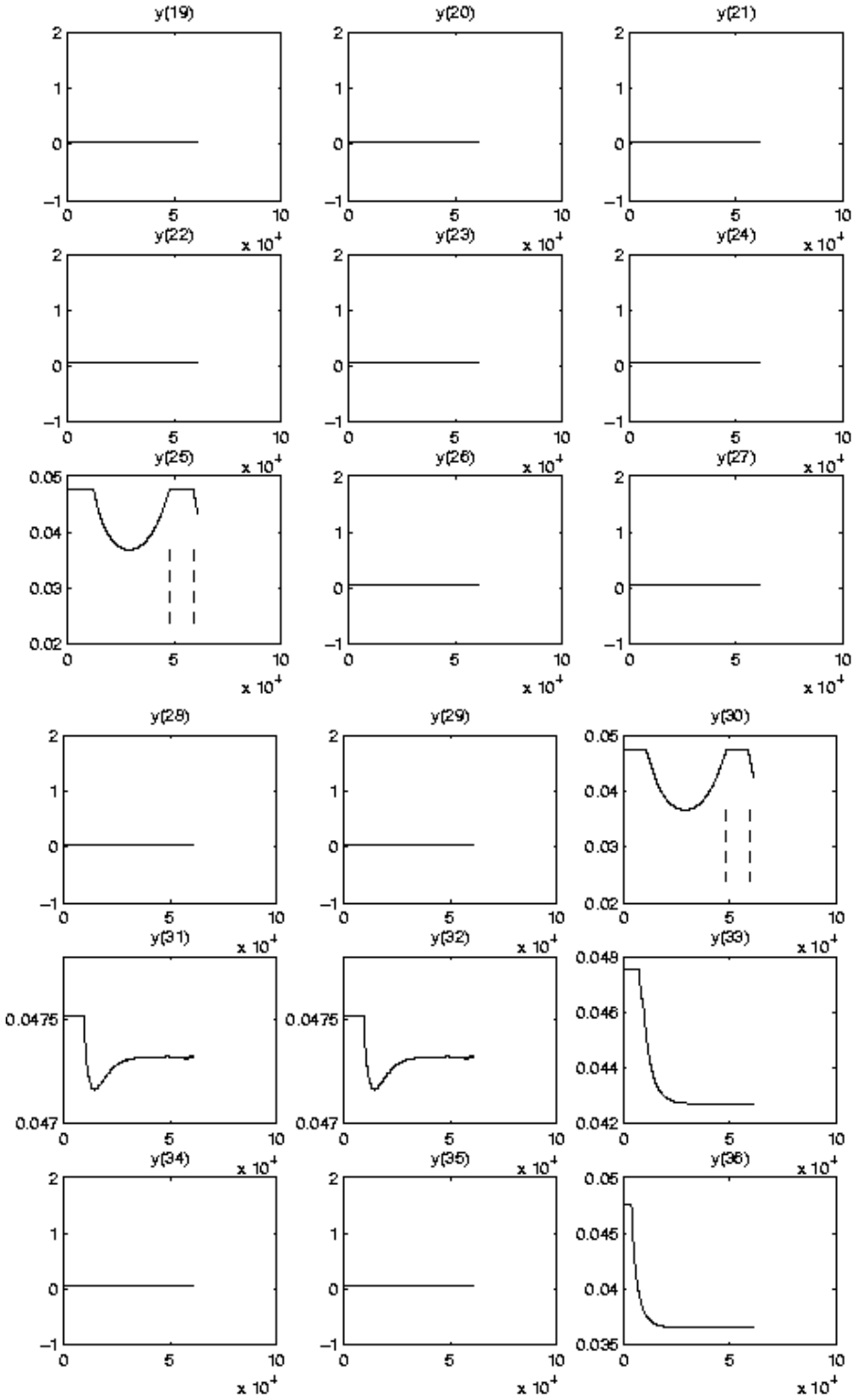

FIGURE II.20.7: *Behavior of resistance coefficients over the integration interval.*

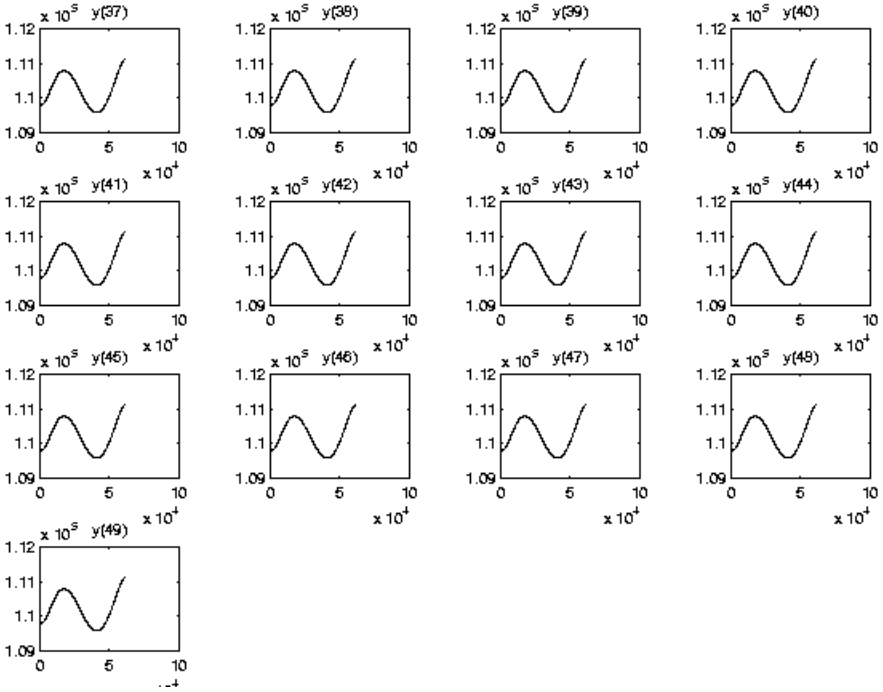

FIGURE II.20.8: *Behavior of pressures over the integration interval.*

TABLE II.20.6: *Failed runs.*

solver	m	reason
RADAU	$0, \ldots 6, 8, 9, 11, 12, 13, 14, 16, \ldots, 20, 24$	solver cannot handle `IERR=-1`.
RADAU5	6	stepsize too small

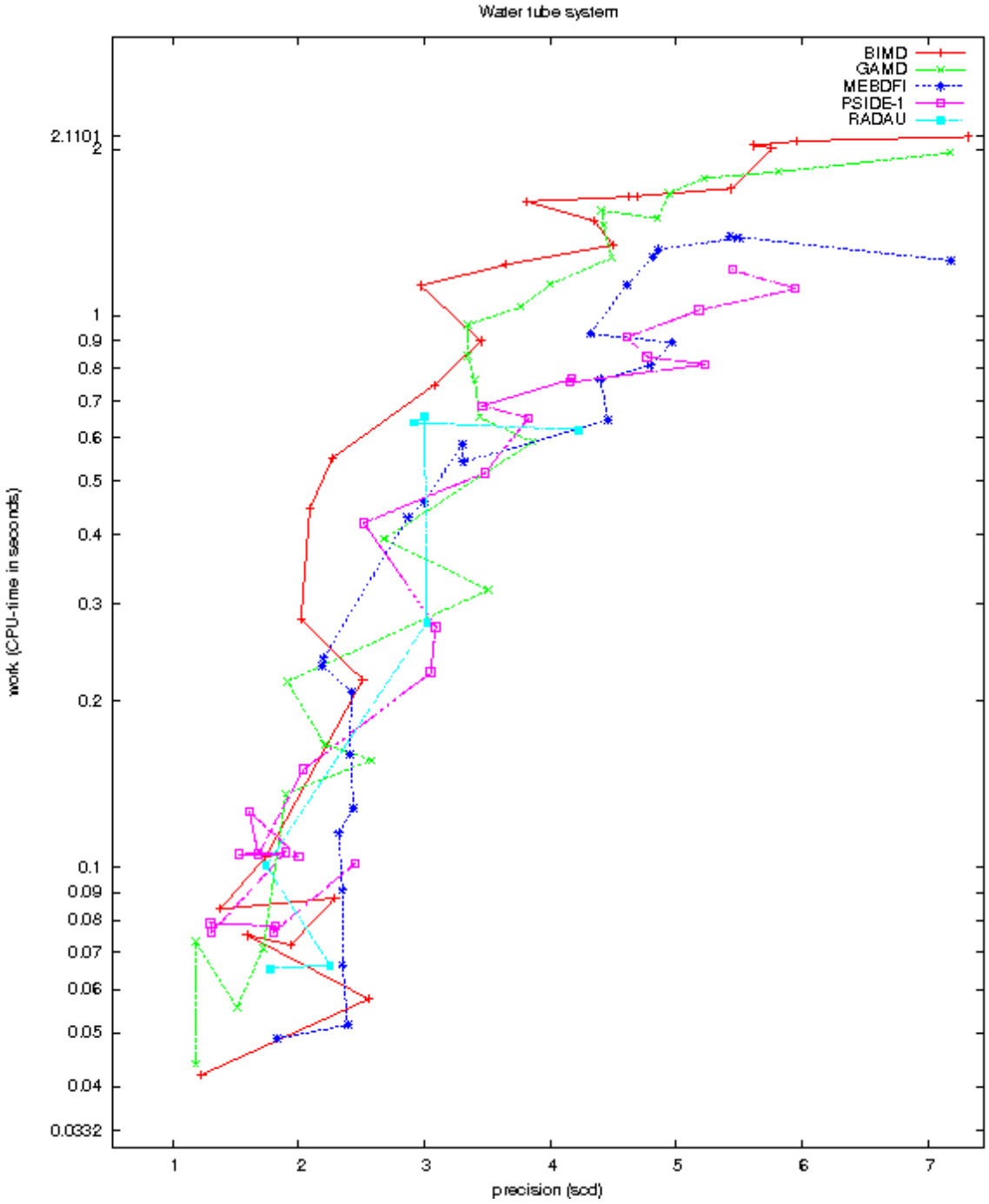

FIGURE II.20.9: *Work-precision diagram (scd versus CPU-time).*

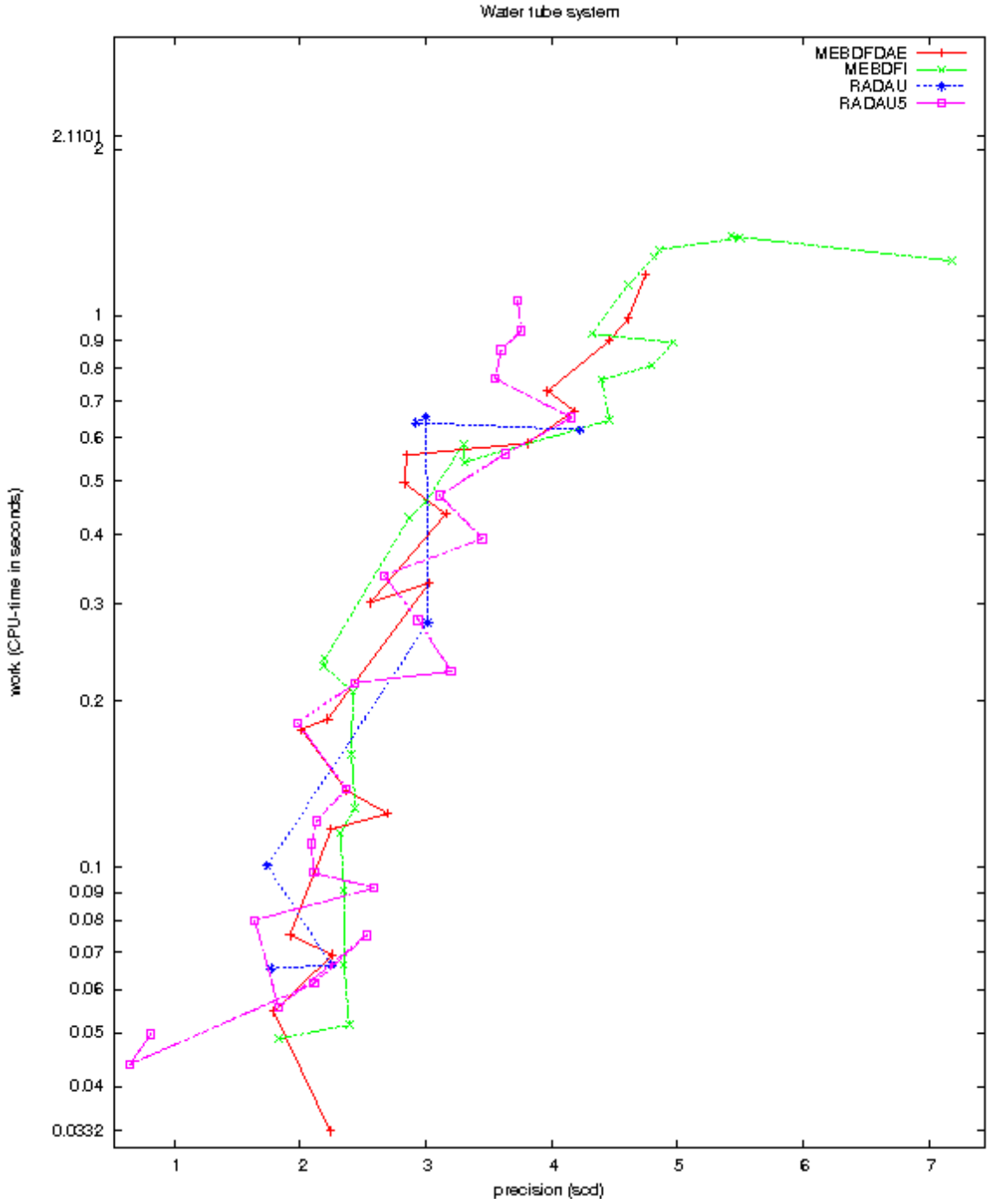

FIGURE II.20.10: *Work-precision diagram (scd versus CPU-time).*

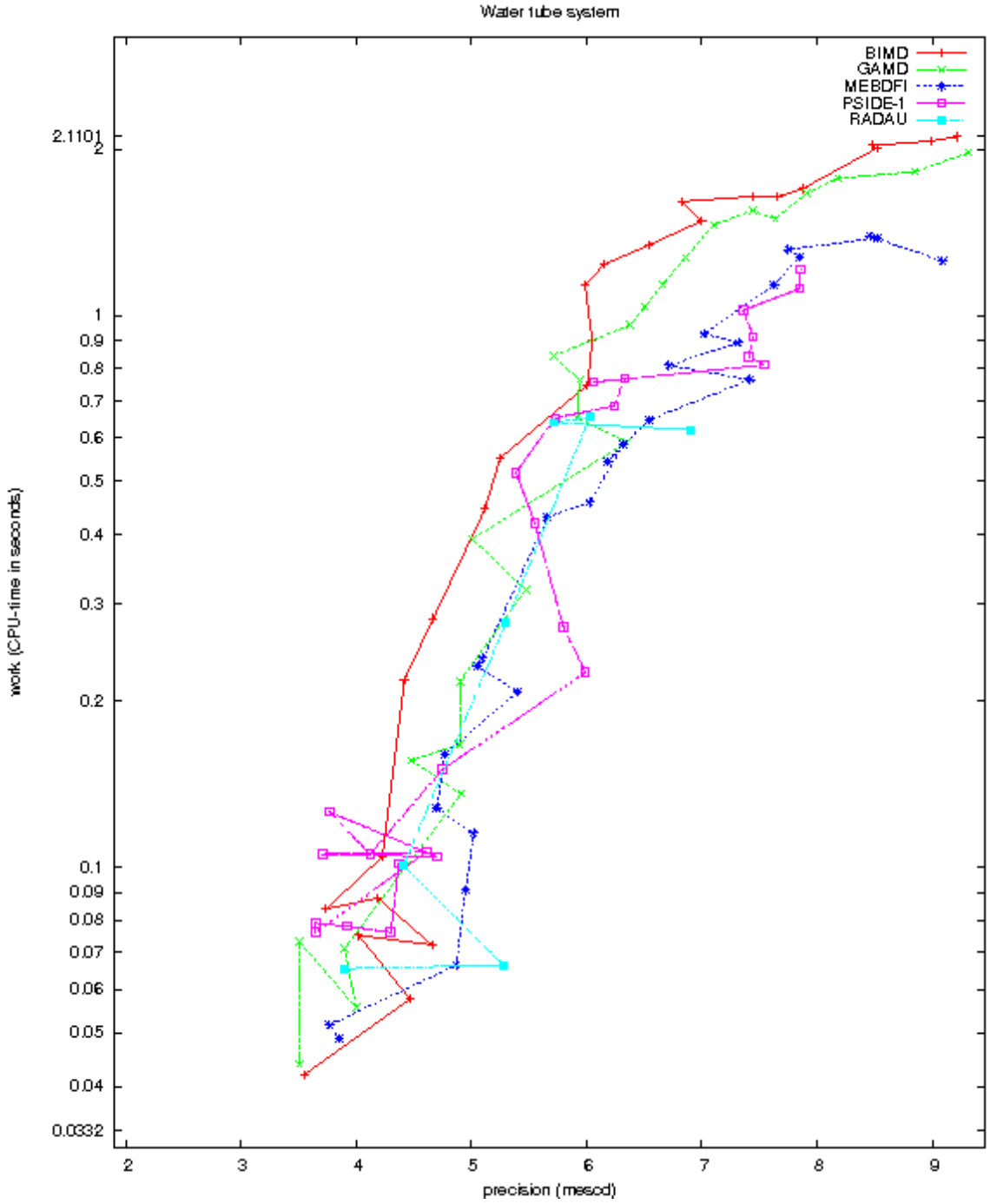

FIGURE II.20.11: *Work-precision diagram (mescd versus CPU-time).*

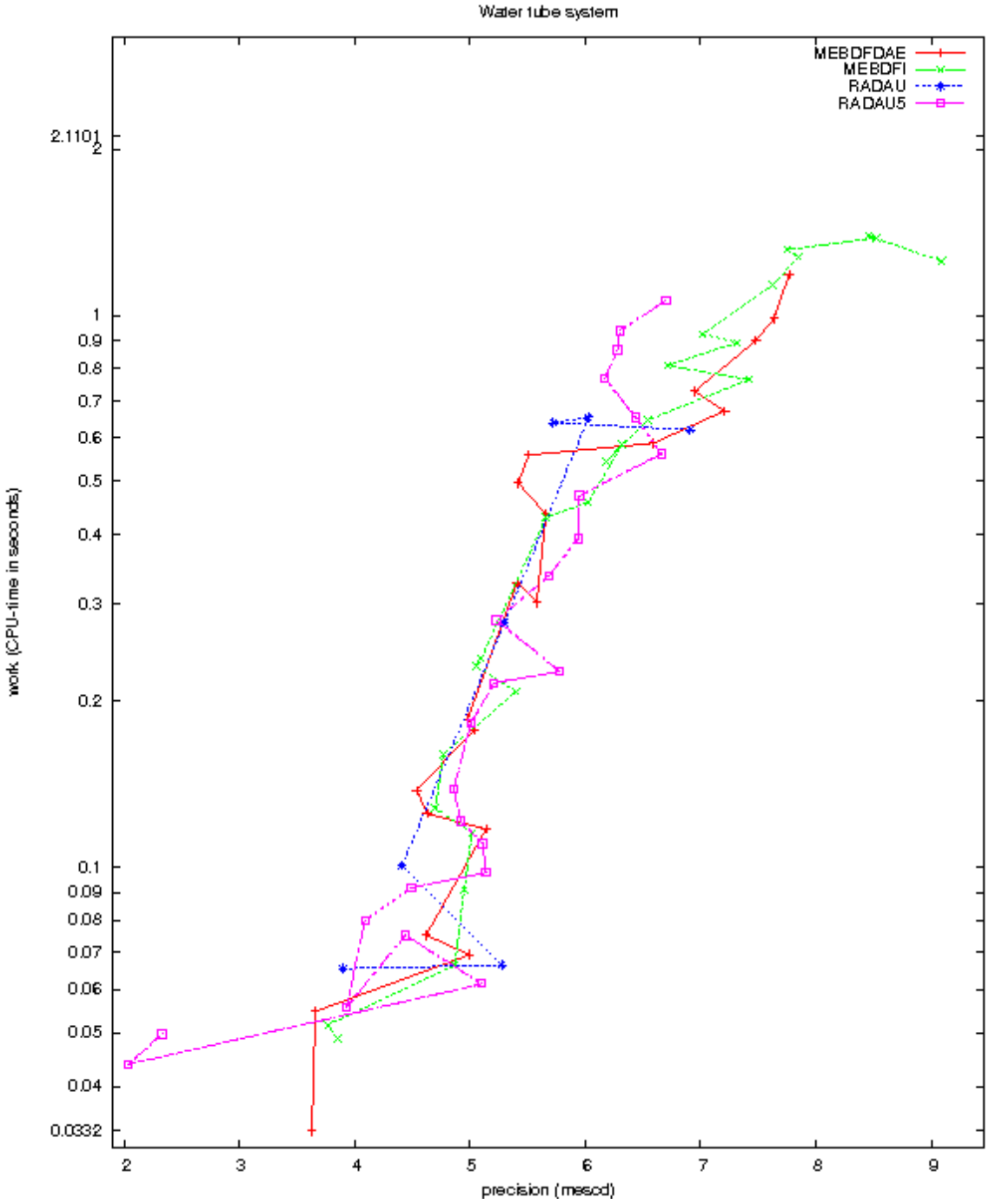

FIGURE II.20.12: *Work-precision diagram (mescd versus CPU-time).*